Okushin K, Asaoka Y, Fukuda I, Fujiwara N, Minami T, Sato M, Mikami S, Uchino K, Enooku K, Kondo Y, Tateishi R, Goto T, Shiina S, Yoshida H, Koike K	IGF-II producing hepatocellular carcinoma treated with sorafenib: metabolic complications and a foresight to molecular targeting therapy to the IGF signal	Case Rep Gastroenterol	6(3)	784-789	2012
Yanagimoto S, Yotsuyanagi H, Kikuchi Y, Tsukada K, Kato M, Takamatsu J, Hige S, Chayama K, Moriya K, Koike K	Chronic hepatitis B in patients coinfected with human immunodeficiency virus in Japan: a retrospective multicenter analysis	J Infect Chemother	18(6)	883-890	2012
Ikeda H, Enooku K, Ohkawa R, Koike K, Yatomi Y	Plasma lysophosphatidic acid levels and hepatocellular carcinoma	Hepatology	57	417-418	2013
Shiina S, Tateishi R, Imamura M, Teratani T, Koike Y, Sato S, Obi S, Kanai F, Kato N, Yoshida H, Omata M, Koike K	Percutaneous ethanol injection for hepatocellular carcinoma: 20-year outcome and prognostic factors	Liver Int	32(9)	1434-1442	2012
Uchino K, Obi S, Tateishi R, Sato S, Kanda M, Sato T, Arano T, Enooku K, Goto E, Masuzaki R, Nakagawa H, Asaoka Y, Kondo Y, Yamashiki N, Goto T, Shiina S, Omata M, Yoshida H, Koike K	Systemic combination therapy of intravenous continuous 5-fluorouracil and subcutaneous pegylated interferon alfa-2a for advanced hepatocellular carcinoma	J Gastroenterol	47(10)	1152-1159	2012

Sato M, Tateishi R, Yasunaga H, Horiguchi H, Yoshida H, Matsuda S, Koike K	Mortality and morbidity of hepatectomy, radiofrequency ablation, and embolization for hepatocellular carcinoma: a national survey of 54,145 patients	J Gastroenterol	47(10)	1125-1133	2012
Yoshikawa T, Takata A, Otsuka M, Kishikawa T, Kojima K, Yoshida H, Koike K	Silencing of microRNA-122 enhances interferon-α signaling in the liver through regulating SOCS3 promoter methylation	Sci Rep	2	637	2012
Nakagawa H, Isogawa A, Tateishi R, Tani M, Yoshida H, Yamakado M, Koike K	Serum gamma-glutamyltransferase level is associated with serum superoxide dismutase activity and metabolic syndrome in a Japanese population	J Gastroenterol	47(2)	187-194	2012
Soroida Y, Ohkawa R, Nakagawa H, Satoh Y, Yoshida H, Kinoshita H, Tateishi R, Masuzaki R, Enooku K, Shiina S, Sato T, Obi S, Hoshino T, Nagatomo R, Okubo S, Yokota H, Koike K, Yatomi Y, Ikeda H	Increased activity of serum mitochondrial isoenzyme of creatine kinase in hepatocellular carcinoma patients predominantly with recurrence	J Hepatol	27(2)	330-336	2012
Takata A, Otsuka M, Yoshikawa T, Kishikawa T, Kudo Y, Goto T, Yoshida H, Koike K	A miRNA machinery component DDX20 controls NF-κB via microRNA-140 function	Biochem Biophys Res Commun	420(3)	564-569	2012

Masuzaki R, Tateishi R, Yoshida H, Arano T, Uchino K, Enooku K, Goto E, Nakagawa H, Asaoka Y, Kondo Y, Goto T, Ikeda H, Shiina S, Omata M, Koike K	Assessment of disease progression in patients with transfusion-associated chronic hepatitis C using transient elastography	World J Gastroenterol	18(12)	1385-1390	2012
Kudo Y, Tateishi K, Yamamoto K, Yamamto S, Asaoka Y, Ijichi H, Nagae G, Yoshida H, Aburatani H, Koike K	Loss of 5-hydroxymethylcytosine is accompanied with malignant cellular transformation	Cancer Sci	103(4)	670-676	2012
Goto E, Masuzaki R, Tateishi R, Kondo Y, Imamura J, Goto T, Ikeda H, Akahane M, Shiina S, Omata M, Yoshida H, Koike K	Value of post-vascular phase (Kupffer imaging) by contrast-enhanced ultrasonography using Sonazoid in the detection of hepatocellular carcinoma	J Gastroenterol	47(4)	47(4)	2012
Shiina S, Tateishi R, Arano T, Uchino K, Enooku K, Nakagawa H, Asaoka Y, Sato T, Masuzaki R, Kondo Y, Goto T, Yoshida H, Omata M, Koike K	Radiofrequency ablation for hepatocellular carcinoma: 10-year outcome and prognostic factors	Am J Gastroenterol	107(4)	569-577	2012
Enooku K, Tateishi R, Kanai F, Kondo Y, Masuzaki R, Goto T, Shiina S, Yoshida H, Omata M, Koike K	Evaluation of molecular targeted cancer drug by changes in tumor marker doubling times	J Gastroenterol	47(1)	71-78	2012

Sawai H, Nishida N, Mbarek H, Matsuda K, Mawatari Y, Yamaoka M, Hige S, Kang JH, Abe K, Mochida S, Watanabe M, Kurosaki M, Asahina Y, Izumi N, Honda M, Kaneko S, Tanaka E, Matsuura K, Itoh Y, Mita E, Korenaga M, Hino K, Murawaki Y, Hiasa Y, Ide T, Ito K, Sugiyama M, Ahn SH, Han KH, Park JY, Yuen MF, Nakamura Y, Tanaka Y, **Mizokami M**, Tokunaga K.	No association for Chinese HBV-related hepatocellular carcinoma susceptibility SNP in other East Asian populations.	BMC Med Genet.	13(1)	47	2012
Nishida N, Sawai H, Matsuura K, Sugiyama M, Ahn SH, Park JY, Hige S, Kang JH, Suzuki K, Kurosaki M, Asahina Y, Mochida S, Watanabe M, Tanaka E, Honda M, Kaneko S, Orito E, Itoh Y, Mita E, Tamori A, Murawaki Y, Hiasa Y, Sakaida I, Korenaga M, Hino K, Ide T, Kawashima M, Mawatari Y, Sageshima M, Ogasawara Y, Koike A, Izumi N, Han KH, Tanaka Y, Tokunaga K, **Mizokami M.**	Genome-wide association study confirming association of HLA-DP with protection against chronic hepatitis B and viral clearance in Japanese and Korean.	PLoS One	7(6)	e39175	2012
Watanabe T, Sugauchi F, Tanaka Y, Matsuura K, Yatsuhashi H, Murakami S, Iijima S, Iio E, Sugiyama M, Shimada T, Kakuni M, Kohara M, **Mizokami M**.	Hepatitis C virus kinetics by administration of pegylated interferon-α in human and chimeric mice carrying human hepatocytes with variants of the IL28B gene.	Gut	In press		2012
Sawada N, Inoue M, Iwasaki M, Sasazuki S, Shimazu T, Yamaji T, Takachi R, Tanaka Y, **Mizokami M**, Tsugane S; Japan Public Health Center-Based Prospective Study Group.	Consumption of n-3 fatty acids and fish reduces risk of hepatocellular carcinoma.	Gastroenterology	142(7)	1468-75	2012

Nishida N, Mawatari Y, Sageshima M, Tokunaga K.	Highly parallel and short-acting amplification with locus-specific primers to detect single nucleotide polymorphisms by the DigiTag2 assay.	PLoS One.	7(1)	e29967	2012
Sawai H, Nishida N, Mbarek H, Matsuda K, Mawatari Y, Yamaoka M, Hige S, Kang JH, Abe K, Mochida S, Watanabe M, Kurosaki M, Asahina Y, Izumi N, Honda M, Kaneko S, Tanaka E, Matsuura K, Itoh Y, Mita E, Korenaga M, Hino K, Murawaki Y, Hiasa Y, Ide T, Ito K, Sugiyama M, Ahn SH, Han KH, Park JY, Yuen MF, Nakamura Y, Tanaka Y, Mizokami M, Tokunaga K.	No association for Chinese HBV-related hepatocellular carcinoma susceptibility SNP in other East Asian populations.	BMC Med Genet	13	47	2012
Nishida N, Sawai H, Matsuura K, Sugiyama M, Ahn SH, Park JY, Hige S, Kang JH, Suzuki K, Kurosaki M, Asahina Y, Mochida S, Watanabe M, Tanaka E, Honda M, Kaneko S, Orito E, Itoh Y, Mita E, Tamori A, Murawaki Y, Hiasa Y, Sakaida I, Korenaga M, Hino K, Ide T, Kawashima M, Mawatari Y, Sageshima M, Ogasawara Y, Koike A, Izumi N, Han KH, Tanaka Y, Tokunaga K, Mizokami M.	Genome-wide association study confirming association of HLA-DP with protection against chronic hepatitis B and viral clearance in Japanese and Korean.	PLoS One	7(6)	e39175	2012

Kumar V, Yi Lo PH, Sawai H, Kato N, Takahashi A, Deng Z, Urabe Y, Mbarek H, Tokunaga K, Tanaka Y, Sugiyama M, Mizokami M, Muroyama R, Tateishi R, Omata M, Koike K, Tanikawa C, Kamatani N, Kubo M, Nakamura Y, Matsuda K.	Soluble MICA and a MICA variation as possible prognostic biomarkers for HBV-induced hepatocellular carcinoma.	Plos One	7(9)	E44743	2012
Kawashima M, Ohashi J, Nishida N, Tokunaga K	Evolutionary analysis of classical HLA class I and II genes suggests that recent positive selection acted on DPB1*04:01 in Japanese population.	PLoS One	7(10)	e46806	2012

Nakamura M, Nishida N, Kawashima M, Aiba Y, Tanaka A, Yasunami M, Nakamura H, Komori A, Nakamuta M, Zeniya M, Hashimoto E, Ohira H, Yamamoto K, Onji M, Kaneko S, Honda M, Yamagiwa S, Nakao K, Ichida T, Takikawa H, Seike M, Umemura T, Ueno Y, Sakisaka S, Kikuchi K, Ebinuma H, Yamashiki N, Tamura S, Sugawara Y, Mori A, Yagi S, Shirabe K, Taketomi A, Arai K, Monoe K, Ichikawa T, Taniai M, Miyake Y, Kumagi T, Abe M, Yoshizawa K, Joshita S, Shimoda S, Honda K, Takahashi H, Hirano K, Takeyama Y, Harada K, Migita K, Ito M, Yatsuhashi H, Fukushima N, Ota H, Komatsu T, Saoshiro T, Ishida J, Kouno H, Kouno H, Yagura M, Kobayashi M, Muro T, Masaki N, Hirata K, Watanabe Y, Nakamura Y, Shimada M, Hirashima N, Komeda T, Sugi K, Koga M, Ario K, Takesaki E, Maehara Y, Uemoto S, Kokudo N, Tsubouchi H, Mizokami M, Nakanuma Y, Tokunaga K, Ishibashi H.	Genome-wide Association Study Identifies TNFSF15 and POU2AF1 as Susceptibility Loci for Primary Biliary Cirrhosis in the Japanese Population.	Am J Hum Genet.	91(4)	721-728	2012
Kurosaki M, Tanaka Y, Nishida N, Sakamoto N, Enomoto N, Matsuura K, Asahina Y, Nakagawa M, Watanabe M, Sakamoto M, Maekawa S, Tokunaga K, Mizokami M, and Izumi N	Model incorporating the ITPA genotype identifies patients at high risk of anemia and treatment failure with pegylated-interferon plus ribavirin therapy for chronic hepatitis C.	J. Med. Viro	85(3)	449-458	2013

Ⅳ. 研究成果の刊行物、別刷

OPEN ACCESS Freely available online

PLOS ONE

Soluble MICA and a *MICA* Variation as Possible Prognostic Biomarkers for HBV-Induced Hepatocellular Carcinoma

Vinod Kumar[1,2]*, Paulisally Hau Yi Lo[1], Hiromi Sawai[3], Naoya Kato[4], Atsushi Takahashi[2], Zhenzhong Deng[1], Yuji Urabe[1], Hamdi Mbarek[1], Katsushi Tokunaga[3], Yasuhito Tanaka[5], Masaya Sugiyama[6], Masashi Mizokami[6], Ryosuke Muroyama[4], Ryosuke Tateishi[7], Masao Omata[7], Kazuhiko Koike[7], Chizu Tanikawa[1], Naoyuki Kamatani[2], Michiaki Kubo[2], Yusuke Nakamura[1], Koichi Matsuda[1]

1 Laboratory of Molecular Medicine, Human Genome Center, Institute of Medical Science, The University of Tokyo, Tokyo, Japan, **2** Center for Genomic Medicine, The Institute of Physical and Chemical Research (RIKEN), Kanagawa, Japan, **3** Department of Human Genetics, Graduate School of Medicine, The University of Tokyo, Tokyo, Japan, **4** Unit of Disease Control Genome Medicine, The Institute of Medical Science, The University of Tokyo, Tokyo, Japan, **5** Department of Clinical Molecular Informative Medicine, Nagoya City University Graduate School of Medical Sciences, Aichi, Japan, **6** The Research Center for Hepatitis and Immunology, National Center for Global Health and Medicine, Chiba, Japan, **7** Department of Gastroenterology, Graduate School of Medicine, The University of Tokyo, Tokyo, Japan

Abstract

MHC class I polypeptide-related chain A (MICA) molecule is induced in response to viral infection and various types of stress. We recently reported that a single nucleotide polymorphism (SNP) rs2596542 located in the *MICA* promoter region was significantly associated with the risk for hepatitis C virus (HCV)-induced hepatocellular carcinoma (HCC) and also with serum levels of soluble MICA (sMICA). In this study, we focused on the possible involvement of MICA in liver carcinogenesis related to hepatitis B virus (HBV) infection and examined correlation between the *MICA* polymorphism and the serum sMICA levels in HBV-induced HCC patients. The genetic association analysis revealed a nominal association with an SNP rs2596542; a G allele was considered to increase the risk of HBV-induced HCC ($P = 0.029$ with odds ratio of 1.19). We also found a significant elevation of sMICA in HBV-induced HCC cases. Moreover, a G allele of SNP rs2596542 was significantly associated with increased sMICA levels ($P = 0.009$). Interestingly, HCC patients with the high serum level of sMICA (>5 pg/ml) exhibited poorer prognosis than those with the low serum level of sMICA (≤5 pg/ml) ($P = 0.008$). Thus, our results highlight the importance of *MICA* genetic variations and the significance of sMICA as a predictive biomarker for HBV-induced HCC.

Citation: Kumar V, Yi Lo PH, Sawai H, Kato N, Takahashi A, et al. (2012) Soluble MICA and a *MICA* Variation as Possible Prognostic Biomarkers for HBV-Induced Hepatocellular Carcinoma. PLoS ONE 7(9): e44743. doi:10.1371/journal.pone.0044743

Editor: Erica Villa, University of Modena & Reggio Emilia, Italy

Received May 3, 2012; **Accepted** August 7, 2012; **Published** September 14, 2012

Funding: This work was conducted as a part of the BioBank Japan Project that was supported by the Ministry of Education, Culture, Sports, Science and Technology of the Japanese government. The funders had no role in study design, data collection and analysis, decision to publish, or preparation of the manuscript.

Competing Interests: The authors have declared that no competing interests exist.

* E-mail: koichima@ims.u-tokyo.ac.jp

Introduction

Hepatocellular carcinoma (HCC) reveals a very high mortality rate that is ranked the third among all cancers in the world [1]. HCC is known to develop in a multistep process which has been related to various risk factors such as genetic factors, environment toxins, alcohol and drug abuse, autoimmune disorders, elevated hepatic iron levels, obesity, and hepatotropic viral infections [2]. Among them, chronic infection with hepatitis B virus (HBV) is one of the major etiological factors for developing HCC with considerable regional variations ranging from 20% of HCC cases in Japan to 65% in China [3].

Interestingly, clinical outcome after the exposure to HBV considerably varies between individuals. The great majority of individuals infected with HBV spontaneously eliminate the viruses, but a subset of patients show the persistent chronic hepatitis B infection (CHB), and then progresses to liver cirrhosis and HCC through a complex interplay between multiple genetic and environmental factors [4]. In this regard, genome wide association studies (GWAS) using single nucleotide polymorphisms (SNPs) have highlighted the importance of genetic factors in the pathogenesis of various diseases including CHB as well as HBV-induced HCC [5,6,7,8,9,10,11,12,13]. Recently, we identified a genetic variant located at 4.7 kb upstream of the *MHC class I polypeptide-related chain A* (*MICA*) gene to be strongly associated with hepatitis C virus (HCV) -induced HCC development [14].

MICA is highly expressed on viral-infected cells or cancer cells, and acts as ligand for NKG2D to activate antitumor effects of Natural killer (NK) cells and $CD8^+$ T cells [15,16]. Our previous results indicated that a G allele of SNP rs2596542 was significantly associated with the lower cancer risk and the higher level of soluble MICA (sMICA) in the serum of HCV-induced HCC patients, demonstrating the possible role of MICA as a tumor suppressor. However, elevation of serum sMICA was shown to be associated with poor prognosis in various cancer patients [17,18,19,20].

Matrix metalloproteinases (MMPs) can cleave MICA at a transmembrane domain [21] and release sMICA proteins from cells. Since sMICA was shown to inhibit the antitumor effects of NK cells and $CD8^+$ T cells by reduction of their affinity to binding to target cells [22,23], the effect of MICA in cancer cells would be modulated by the expression of MMPs. To elucidate the role of MICA in HBV-induced hepatocellular carcinogenesis, we here report analysis of the *MICA* polymorphism and serum sMICA level in HBV-induced HCC cases.

Materials and Methods

Study participants

The demographic details of study participants are summarized in Table 1. A total of 181 HCC cases, 597 CHB patients, and 4,549 non-HBV controls were obtained from BioBank Japan that was initiated in 2003 with the funding from the Ministry of Education, Culture, Sports, Science and Technology, Japan [24]. In the Biobank Japan Project, DNA and serum of patients with 47 diseases were collected through collaborating network of 66 hospitals throughout Japan. List of participating hospitals is shown in the following website (http://biobankjp.org/plan/member_hospital.html). A total of 226 HCC cases, 102 CHB patients, and 174 healthy controls were additionally obtained from the University of Tokyo. The diagnosis of chronic hepatitis B was conducted on the basis of HBsAg-seropositivity and elevated serum aminotransferase levels for more than six months according to the guideline for diagnosis and treatment of chronic hepatitis (The Japan Society of Hepatology, http://www.jsh.or.jp/medical/gudelines/index.html). Control Japanese DNA samples (n = 934) were obtained from Osaka-Midosuji Rotary Club, Osaka, Japan. All HCC patients were histopathologically diagnosed. Overall survival was defined as the time from blood sampling for sMICA test to the date of death due to HCC. Patients who were alive on the date of last follow-up were censored on that date. All participants provided written informed consent. This research project was approved by the ethics committee of the University of Tokyo and the ethics committee of RIKEN. All clinical assessments and specimen collections were conducted according to Declaration of Helsinki principles.

SNP genotyping

Genotyping platforms used in this study were shown in Table 1. We genotyped 181 HCC cases and 5,483 non-HBV control samples using either Illumina Human Hap610-Quad or Human Hap550v3. The other samples were genotyped at SNP rs2596542 by the Invader assay system (Third Wave Technologies, Madison, WI).

MICA variable number tandem repeat (VNTR) locus genotyping

Genotyping of the *MICA* VNTR locus in 176 HBV-induced HCC samples was performed using the primers reported previously by the method recommended by Applied Biosystems (Foster City, CA) [14]. Briefly, the 5′ end of forward primer was labeled with 6-FAM, and reverse primer was modified with GTGTCTT non-random sequence at the 5′ end to promote Plus A addition. The PCR products were mixed with Hi-Di Formamide and GeneScan-600 LIZ size standard, and separated by GeneScan system on a 3730×l DNA analyzer (Applied Biosystems, Foster City, CA). GeneMapper software (Applied Biosystems, Foster City, CA) was employed to assign the repeat fragment size (Figure S1).

Quantification of soluble MICA

We obtained serum samples of 111 HBV-positive HCC samples, 129 HCV-positive HCC samples, and 60 non-HBV controls from Biobank Japan. Soluble MICA levels were measured by sandwich enzyme-linked immunosorbent assay, as described in the manufacturer's instructions (R&D Systems, Minneapolis, MN).

Statistical analysis

The association between an SNP rs2596542 and HBV-induced HCC was tested by Cochran-Armitage trend test. The Odds ratios were calculated by considering a major allele as a reference. Statistical comparisons between genotypes and sMICA levels were performed by Kruskal-Wallis test (if more than two classes for comparison) or Wilcoxon rank test using R. Overall survival rate of the patients was analyzed by Kaplan-Meier method in combination with log-rank test with SPSS 20 software. The period for the survival analysis was calculated from the date of blood sampling to the recorded date of death or the last follow-up date. Differences with a P value of <0.05 were considered statistically significant.

Results

Association of SNP rs2596542 with HBV-induced HCC

In order to examine the effect of rs2596542 genotypes on the susceptibility to HBV-induced HCC, a total of 407 HCC cases and 5,657 healthy controls were genotyped. The Cochran Armitage trend test of the data revealed a nominal association

Table 1. Demographic details of subjects analyzed.

Subjects	Source	Genotyping platform	Number of Sample	Female (%)	Age (mean+/−sd)
Liver Cancer	BioBank Japan	Illumina Human Hap610-Quad	181	17.9	62.94±9.42
	University of Tokyo	Invader assay	226		
Control	BioBank Japan	Illumina Human Hap550v3	4549	47.95	55.19±12.5
	Osaka**	Illumina Human Hap550v3	934		
	University of Tokyo	Invader assay	174		
Chronic hepatitis B*	BioBank Japan	Invader assay	597	45.66	61.31±12.6
	University of Tokyo	Invader assay	102		

*Chronic hepatitis B patients without liver cirrhosis and liver cancer during enrollment.
**Healthy volunteers from Osaka Midosuji Rotary Club, Osaka, Japan.
doi:10.1371/journal.pone.0044743.t001

between HBV-induced HCC and rs2596542 in which a risk allele G was more frequent among HBV-induced HCC cases than an A allele (P = 0.029, OR = 1.19, 95% CI: 1.02–1.4; Table 2). To further investigate the effect of rs2596542 on the progression from CHB to HBV-induced HCC, we genotyped a total of 699 CHB cases without HCC. Although the progression risk from CHB to HBV-induced HCC was not statistically significant with rs2596542 (P = 0.197 by the Cochran Armitage trend test with an allelic OR = 1.3 (0.94–1.36); Table 2), we found a similar trend of association in which the frequency of a risk-allele G was higher among HBV-induced HCC patients than that of CHB subjects. Since we previously revealed that an A allele was associated with a higher risk of HCV-induced HCC with OR of 1.36 [14], the s2596542 alleles that increased the risk of HCC were opposite in HBV-induced HCC and HCV-induced HCC.

Soluble MICA levels are associated with SNP rs2596542

We subsequently performed measurement of soluble MICA (sMICA) in serum samples using the ELISA method in 176 HBV-positive HCC cases and 60 non-HBV controls. Nearly 30% of the HBV-induced HCC cases revealed the serum sMICA level of >5 pg/ml (defined as high) while the all control individuals except one showed that of ≤5 pg/ml (defined as low) ($P = 4.5 \times 10^{-6}$; Figure 1A). Then, we examined correlation between SNP rs2596542 genotypes and serum sMICA levels in HBV-positive HCC cases. Interestingly, rs2596542 genotypes were significantly associated with serum sMICA levels (P = 0.009; Figure 1B); 39% of individuals with the GG genotype and 20% of those with the AG genotype were classified as high for serum sMICA, but only 11% of those with the AA genotype were classified as high (AA+AG vs GG; P = 0.003) (Figure 1B). These findings were similar with our previous reports in which a G allele was associated with higher serum sMICA levels in HCV-induced HCC patients [14].

Negative association of variable number of tandem repeat (VNTR) with sMICA level

The *MICA* gene harbors a VNTR locus in exon 5 that consists of 4, 5, 6, or 9 repeats of GCT as well as a G nucleotide insertion into a five-repeat allele (referred as A4, A5, A6, A9, and A5.1, respectively). The insertion of G (A5.1) causes a premature translation termination and results in loss of a transmembrane domain, which may produce the shorter form of the MICA protein that is likely be secreted into serum [25]. However, the association of this VNTR locus with serum sMICA level was controversial among studies [14,26,27,28]. Therefore, we examined the association between the VNTR locus and sMICA level in HBV-induced HCC patients, and found no significant association (Figure S1 and S2), concordant with our previous report for HCV-induced HCC patients [14].

Soluble MICA levels are associated with survival of HCC patients

In order to evaluate the prognostic significance of serum sMICA levels in HCC patients, we performed survival analysis of HCC patients. A total of 111 HBV-infected HCC patients and 129 HCV-infected HCC patients were included in this analysis. The mean survival period for HBV- and HCV-infected patients with less than 5 pg/ml of serum sMICA were 67.1 months (95% CI: 61.1–73.1, n = 83), and 58.2 months (95% CI: 51.4–65.0, n = 85), respectively. On the other hand, for patients with more than 5 pg/ml of serum sMICA, the mean survival periods were 47.8 months (95% CI: 34.8–30.9, n = 28) for HBV-induced HCC patients and 59.5 months (95% CI: 51.9–67.1, n = 44) for HCV-induced HCC patients. The Kaplan-Maier analysis and log-rank test indicated that among HBV-induced HCC subjects, the patients in the high serum sMICA group showed a significantly shorter survival than those in the low serum sMICA (P = 0.008; Figure 2). In addition, we performed multi-variate analysis to test whether sMICA is an independent prognostic factor by including age and gender as covariates. The results revealed significant association of sMICA levels with overall survival (P = 0.017) but not with age and gender (Table S1).However, we found no association between the serum sMICA level and the overall survival in the HCV-induced HCC subjects (P = 0.414; Figure S3). Taken together, our findings imply the distinct roles of the *MICA* variation and sMICA between HBV- and HCV-induced hepatocellular carcinogenesis.

Vascular invasion in HBV-related HCC patients is associated with soluble MICA levels

Since sMICA levels were associated with the overall survival of HBV-related HCC patients, we tested whether sMICA levels affect survival through modulating invasive properties of tumors or size of the tumors. We tested the association between sMICA levels and vascular invasion in 35 HBV-related HCC cases, among whom 7 cases were positive and 21 cases were negative for vascular invasion. We found significant association between sMICA levels and vascular invasion (Figure 3; P = 0.014) in which 7 cases with positive vascular invasion showed high levels of sMICA (mean = 54 pg/ml) than 21 cases without vascular invasion (mean = 7.51 pg/ml). However, we found no association between tumor size and sMICA levels (P = 0.56; data not shown). These results suggest that sMICA may reduce the survival of HBV-related HCC patients by affecting the invasive properties of tumors.

Discussion

Several mechanisms such as HBV-genome integration into host chromosomal DNA [29] and effects of viral proteins including HBx [30] are shown to contribute to development and progression of HCC, while the immune cells such as NK and T cells function as key antiviral and antitumor effectors. MICA protein has been

Table 2. Association between HCC and rs2596542.

SNP	Comparison	Chr	Locus	Case MAF	Control MAF	P*	OR*	95% CI
rs2596542	HCC vs. Healthy control	6	*MICA*	0.294	0.332	0.029	1.19	1.02–1.4
rs2596542	HCC vs. CHB	6	*MICA*	0.294	0.320	0.197	1.13	0.94–1.36

Note: 407 HCC cases, 699 CHB subjects and 5,657 non-HBV controls were used in the analysis.
Chr.,chromosome; MAF, minor allele frequency; OR, odds ratio for minor allele; CI, confidence interval.
*Obtained by Armitage trend test.
doi:10.1371/journal.pone.0044743.t002

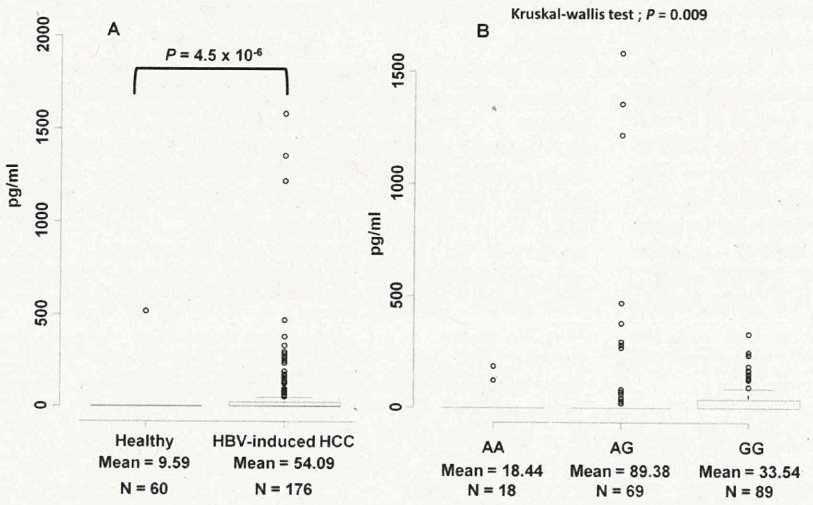

Figure 1. Soluble MICA levels are associated with HBV-related HCC. (A) Correlation between soluble MICA levels and HBV-induced HCC subjects. The y-axis displays the concentration of soluble MICA in pg/ml. The number of independent samples tested in each group is shown in the x-axis. Each group is shown as a box plot and the mean values are shown in the x-axis. The difference between two groups is tested by Wilcoxon rank test. The box plots are plotted using default settings in R. (B) Correlation between soluble MICA levels and rs2596542 genotype in HBV-positive HCC subjects. The x-axis shows the genotypes at rs2596542 and y-axis display the concentration of soluble MICA in pg/ml. Each group is shown as a box plot. $P = 0.027$ and 0.013 for AA vs. GG and AA vs. AG, respectively. The association between genotypes and sMICA levels was tested by Kruskal-wallis test, whereas the difference in the sMICA levels between AA and GG is tested by Wilcoxon rank test. The box plots are plotted using default settings in R.
doi:10.1371/journal.pone.0044743.g001

considered as a stress marker of gastrointestinal epithelial cells because of its induced expression by several external stimuli such as heat, DNA damage, and viral infections [31,32,33,34]. Here, we examined the association of rs2596542 and serum sMICA levels with HBV-induced HCC. Like in HCV-induced HCC [14], our results from ELISA revealed a significantly higher proportion

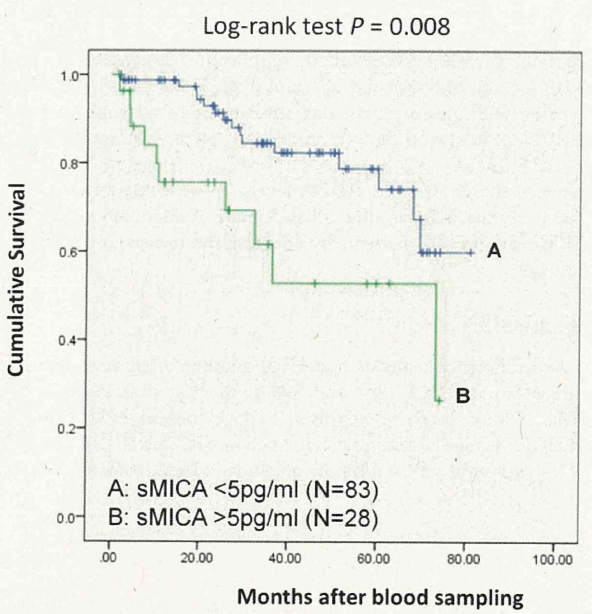

Figure 2. Kaplan-Meier curves of the patients with HBV-induced HCC. The patients were divided into two groups according to their sMICA concentration (high: >5 pg/ml and low: =<5 pg/ml). Statistical difference was analyzed by log-rank test. The y-axis shows the cumulative survival probability and x-axis display the months of the patients survival after blood sampling.
doi:10.1371/journal.pone.0044743.g002

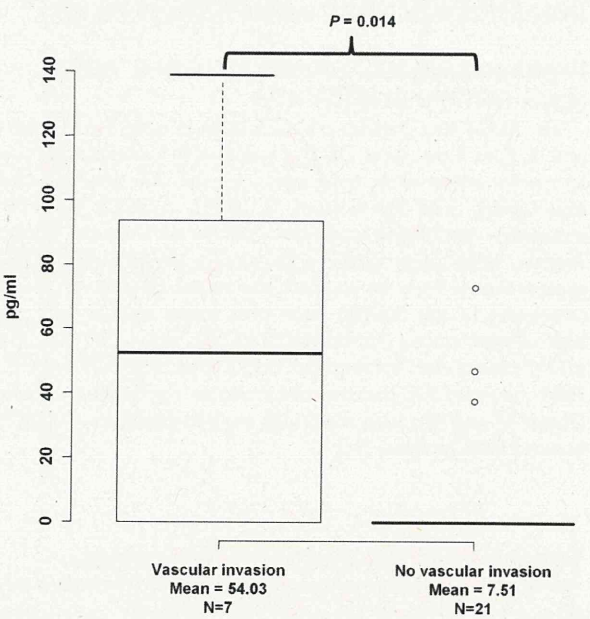

Figure 3. Correlation between soluble MICA levels and vascular invasion in HBV-induced HCC subjects. The y-axis displays the concentration of soluble MICA in pg/ml. The number of independent samples tested in each group is shown in the x-axis. Each group is shown as a box plot and the mean values are shown in the x-axis. The difference between two groups is tested by Wilcoxon rank test. The box plots are plotted using default settings in R.
doi:10.1371/journal.pone.0044743.g003

of high serum sMICA cases (nearly 30%) in the HBV-induced HCC group, compared to non-HBV individuals (1.7%). Moreover, the serum sMICA level was significantly associated with rs2596542, but not with the copy number differences of the VNTR locus, as concordant with our previous report [14].

Several studies have already indicated the roles of sMICA as prognostic markers for different types of malignant diseases [17,18,19,20]. Therefore, it is of medical importance to test whether serum sMICA levels can be used as a prognostic marker for patients with HCC. To our best knowledge, this is the first study to demonstrate the prognostic potential of sMICA for HBV-positive HCC patients; we found 19.3 months of improvement in survival among patients carrying less than 5 pg/ml of serum sMICA, compared to those having more than 5 pg/ml.

On the contrary, we found no significant correlation between sMICA levels and the prognosis of HCV-induced HCC cases. These opposite effects of *MICA* variation could be explained by the following mechanism. The individuals who carry the G allele would express high levels of membrane-bound MICA upon HCV infection and thus lead to the activation of immune cells against virus infected cells. On one hand, HBV infection results in increased expression of membrane-bound MICA as well as MMPs through viral protein HBx [35], which would result in the elevation of sMICA and the reduction of membrane-bound MICA. Since sMICA could block CD8+T cells, NK-CTL, and NK cells, higher sMICA would cause the inactivation of immune surveillance system against HBV infected cells. In other words, HBV may use this strategy to evade immune response and hence, higher levels of sMICA could be associated with lower survival rate among HBV-associated HCC. On the other hand, since HCV is not known to induce the cleavage of membrane bound MICA, individuals with low level membrane bound MICA expression (carriers of rs2596542-allele A) could be inherently susceptible for HCV-induced HCC. Thus, HBx-medicated induction of MMPs could partially explain the intriguing contradictory effect of MICA between HBV-induced HCC and HCV-induced HCC. Since we observed significant correlation of sMICA levels with vascular invasion, it may be the case that high levels of sMICA cause poor prognosis of HBV-related HCC cases by making tumors more aggressive and invasive. However it is important in future to determine the ratio of membrane-bound MICA to sMICA in case of HCV- and HBV-related HCC.

Interestingly, the immune therapy against melanoma patients induced the production of auto-antibodies against MICA [36]. Anti-MICA antibodies would exert antitumor effects through antibody-dependent cellular cytotoxicity against cells expressing membrane-bound MICA and/or activation of NK cells by inhibiting the sMICA-NKG2D interaction. However, further studies are necessary, using well-defined HBV-related HCC cohort, to investigate whether sMICA levels could be included as an additional factor to predict the survival rate among HBV-related HCC subjects. Taken together, our results indicate the potential of *MICA* variant and sMICA as prognostic biomarkers. Thus, MICA could be a useful therapeutic target for HBV-induced HCC.

Supporting Information

Figure S1 MICA repeat genotyping using capillary-based method. The alleles are annotated using GeneMapper software based on the size of the PCR product (185 bp = A4 allele, 188 bp = A5, 189 bp = A5.1, 191 bp = A6 and 200 bp = A9). The inset at the base of each peak shows the size of the PCR product with corresponding allele call by the software. The figure display all observed heterozygotes at A5.1 allele.
(TIF)

Figure S2 MICA VNTR alleles are not associated with soluble MICA levels. Each group is shown as a box plot. The difference in the sMICA values among each group is tested by Wilcoxon rank test. The box plots are plotted using default settings in R.
(TIF)

Figure S3 Kaplan-Meier curves of the patients with HCV-induced HCC. The patients were divided into two groups according to their sMICA concentration (<5 pg/ml or >5 pg/ml). Statistical difference was analyzed by log-rank test. The y-axis shows the cumulative survival probability and x-axis display the months of the patients survival after blood sampling.
(TIF)

Table S1 Clinical parameters of HBV-related HCC patients available for prognostic analyses.
(XLS)

Acknowledgments

We would like to thank all the patients and the members of the Rotary Club of Osaka-Midosuji District 2660 Rotary International in Japan, who donated their DNA for this work. We also thank Ayako Matsui and Hiroe Tagaya (the University of Tokyo), and the technical staff of the Laboratory for Genotyping Development, Center for Genomic Medicine, RIKEN for their technical support.

Author Contributions

Conceived and designed the experiments: VK KM YN. Performed the experiments: VK PHL YU HM ZD. Analyzed the data: VK PHL CT RM. Contributed reagents/materials/analysis tools: YN NK AT MK HS KT YT MS MM RT MO KK NK. Wrote the paper: VK PHL KM YN.

References

1. Kew MC (2010) Epidemiology of chronic hepatitis B virus infection, hepatocellular carcinoma, and hepatitis B virus-induced hepatocellular carcinoma. Pathol Biol (Paris) 58: 273–277.
2. Sherman M (2010) Hepatocellular carcinoma: epidemiology, surveillance, and diagnosis. Semin Liver Dis 30: 3–16.
3. Perz J, Armstrong G, Farrington L, Hutin Y, Bell B (2006) The contributions of hepatitis B virus and hepatitis C virus infections to cirrhosis and primary liver cancer worldwide. J Hepatol 45: 529–538.
4. Chen CJ, Chen DS (2002) Interaction of hepatitis B virus, chemical carcinogen, and genetic susceptibility: multistage hepatocarcinogenesis with multifactorial etiology. Hepatology 36: 1046–1049.
5. Cui R, Okada Y, Jang SG, Ku JL, Park JG, et al. (2011) Common variant in 6q26–q27 is associated with distal colon cancer in an Asian population. Gut 60: 799–805.
6. Kumar V, Matsuo K, Takahashi A, Hosono N, Tsunoda T, et al. (2011) Common variants on 14q32 and 13q12 are associated with DLBCL susceptibility. J Hum Genet England. pp. 436–439.
7. Cui R, Kamatani Y, Takahashi A, Usami M, Hosono N, et al. (2009) Functional variants in ADH1B and ALDH2 coupled with alcohol and smoking synergistically enhance esophageal cancer risk. Gastroenterology 137: 1768–1775.
8. Urabe Y, Tanikawa C, Takahashi A, Okada Y, Morizono T, et al. (2012) A genome-wide association study of nephrolithiasis in the Japanese population identifies novel susceptible loci at 5q35.3, 7p14.3 and 13q14.1. PLOS Genet 8(3): e1002541.
9. Tanikawa C, Urabe Y, Matsuo K, Kubo M, Takahashi A, et al. (2012) A genome-wide association study identifies two susceptibility loci for duodenal ulcer in the Japanese population. Nat Genet 44(4): 430–434.

10. Hata J, Matsuda K, Ninomiya T, Yonemoto K, Matsushita T, et al. (2007) Functional SNP in an Sp1-binding site of AGTRL1 gene is associated with susceptibility to brain infarction. Hum Mol Genet 16: 630–639.
11. Kamatani Y, Wattanapokayakit S, Ochi H, Kawaguchi T, Takahashi A, et al. (2009) A genome-wide association study identifies variants in the HLA-DP locus associated with chronic hepatitis B in Asians. Nat Genet 41: 591–595.
12. Mbarek H, Ochi H, Urabe Y, Kumar V, Kubo M, et al. (2011) A genome-wide association study of chronic hepatitis B identified novel risk locus in a Japanese population. Human Molecular Genetics 20: 3884–3892.
13. Zhang H, Zhai Y, Hu Z, Wu C, Qian J, et al. (2010) Genome-wide association study identifies 1p36.22 as a new susceptibility locus for hepatocellular carcinoma in chronic hepatitis B virus carriers. Nat Genet 42: 755–758.
14. Kumar V, Kato N, Urabe Y, Takahashi A, Muroyama R, et al. (2011) Genome-wide association study identifies a susceptibility locus for HCV-induced hepatocellular carcinoma. Nature genetics 43: 455–458.
15. Jinushi M, Takehara T, Tatsumi T, Kanto T, Groh V, et al. (2003) Expression and role of MICA and MICB in human hepatocellular carcinomas and their regulation by retinoic acid. Int J Cancer 104: 354–361.
16. Bauer S, Groh V, Wu J, Steinle A, Phillips JH, et al. (1999) Activation of NK cells and T cells by NKG2D, a receptor for stress-inducible MICA. Science 285: 727–729.
17. Holdenrieder S, Stieber P, Peterfi A, Nagel D, Steinle A, et al. (2006) Soluble MICA in malignant diseases. Int J Cancer 118: 684–687.
18. Nückel H, Switala M, Sellmann L, Horn PA, Dürig J, et al. (2010) The prognostic significance of soluble NKG2D ligands in B-cell chronic lymphocytic leukemia. Leukemia 24: 1152–1159.
19. Tamaki S, Sanefuzi N, Kawakami M, Aoki K, Imai Y, et al. (2008) Association between soluble MICA levels and disease stage IV oral squamous cell carcinoma in Japanese patients. Hum Immunol 69: 88–93.
20. Li K, Mandai M, Hamanishi J, Matsumura N, Suzuki A, et al. (2009) Clinical significance of the NKG2D ligands, MICA/B and ULBP2 in ovarian cancer: high expression of ULBP2 is an indicator of poor prognosis. Cancer Immunol Immunother 58: 641–652.
21. Salih H, Rammensee H, Steinle A (2002) Cutting edge: down-regulation of MICA on human tumors by proteolytic shedding. J Immunol 169: 4098–4102.
22. Groh V, Wu J, Yee C, Spies T (2002) Tumour-derived soluble MIC ligands impair expression of NKG2D and T-cell activation. Nature 419: 734–738.
23. Jinushi M, Takehara T, Tatsumi T, Hiramatsu N, Sakamori R, et al. (2005) Impairment of natural killer cell and dendritic cell functions by the soluble form of MHC class I-related chain A in advanced human hepatocellular carcinomas. J Hepatol 43: 1013–1020.
24. Nakamura Y (2007) The BioBank Japan Project. Clin Adv Hematol Oncol 5: 696–697.
25. Ota M, Katsuyama Y, Mizuki N, Ando H, Furihata K, et al. (1997) Trinucleotide repeat polymorphism within exon 5 of the MICA gene (MHC class I chain-related gene A): allele frequency data in the nine population groups Japanese, Northern Han, Hui, Uygur, Kazakhstan, Iranian, Saudi Arabian, Greek and Italian. Tissue Antigens 49: 448–454.
26. Tamaki S, Sanefuzi N, Ohgi K, Imai Y, Kawakami M, et al. (2007) An association between the MICA-A5.1 allele and an increased susceptibility to oral squamous cell carcinoma in Japanese patients. J Oral Pathol Med 36: 351–356.
27. Tamaki S, Kawakami M, Yamanaka Y, Shimomura H, Imai Y, et al. (2009) Relationship between soluble MICA and the MICA A5.1 homozygous genotype in patients with oral squamous cell carcinoma. Clin Immunol 130: 331–337.
28. Lü M, Xia B, Ge L, Li Y, Zhao J, et al. (2009) Role of major histocompatibility complex class I-related molecules A*A5.1 allele in ulcerative colitis in Chinese patients. Immunology 128: e230–236.
29. Bonilla Guerrero R, Roberts LR (2005) The role of hepatitis B virus integrations in the pathogenesis of human hepatocellular carcinoma. J Hepatol 42: 760–777.
30. Bouchard MJ, Schneider RJ (2004) The enigmatic X gene of hepatitis B virus. J Virol 78: 12725–12734.
31. Groh V, Bahram S, Bauer S, Herman A, Beauchamp M, et al. (1996) Cell stress-regulated human major histocompatibility complex class I gene expressed in gastrointestinal epithelium. Proc Natl Acad Sci U S A 93: 12445–12450.
32. Groh V, Steinle A, Bauer S, Spies T (1998) Recognition of stress-induced MHC molecules by intestinal epithelial gammadelta T cells. Science 279: 1737–1740.
33. Groh V, Rhinehart R, Randolph-Habecker J, Topp M, Riddell S, et al. (2001) Costimulation of CD8alphabeta T cells by NKG2D via engagement by MIC induced on virus-infected cells. Nat Immunol 2: 255–260.
34. Gasser S, Orsulic S, Brown EJ, Raulet DH (2005) The DNA damage pathway regulates innate immune system ligands of the NKG2D receptor. Nature 436: 1186–1190.
35. Lara-Pezzi E, Gomez-Gaviro MV, Galvez BG, Mira E, Iniguez MA, et al. (2002) The hepatitis B virus X protein promotes tumor cell invasion by inducing membrane-type matrix metalloproteinase-1 and cyclooxygenase-2 expression. J Clin Invest 110: 1831–1838.
36. Jinushi M, Hodi F, Dranoff G (2006) Therapy-induced antibodies to MHC class I chain-related protein A antagonize immune suppression and stimulate antitumor cytotoxicity. Proc Natl Acad Sci U S A 103: 9190–9195.

GENES, CHROMOSOMES & CANCER 52:126–139 (2013)

RESEARCH ARTICLES

The Histone Methyltransferase Wolf–Hirschhorn Syndrome Candidate 1-Like 1 (WHSC1L1) Is Involved in Human Carcinogenesis

Daechun Kang,[1] Hyun-Soo Cho,[1] Gouji Toyokawa,[1,2] Masaharu Kogure,[1] Yuka Yamane,[1] Yukiko Iwai,[1] Shinya Hayami,[1] Tatsuhiko Tsunoda,[3] Helen I. Field,[4] Koichi Matsuda,[1] David E. Neal,[5] Bruce A. J. Ponder,[5] Yoshihiko Maehara,[2] Yusuke Nakamura,[1,6] and Ryuji Hamamoto[1,5]*

[1]Laboratory of Molecular Medicine, Human Genome Center, Institute of Medical Science, The University of Tokyo, Minato-ku, Tokyo 108-8639, Japan
[2]Department of Surgery and Science, Graduate School of Medical Science, Kyusyu University, Higashi-ku, Fukuoka 812-8582, Japan
[3]Laboratory for Medical Informatics, RIKEN, Yokohama, Kanagawa 230-0045, Japan
[4]Department of Genetics, University of Cambridge, Cambridge CB23EH, UK
[5]Department of Oncology, Cancer Research UK Cambridge Research Institute, University of Cambridge, Cambridge CB2 0RE, UK
[6]Section of Hematology/Oncology, The University of Chicago, Chicago, IL 60637

Histone lysine methylation plays a fundamental role in chromatin organization. Although a set of histone methyltransferases have been identified and biochemically characterized, the pathological roles of their dysfunction in human cancers are still not well understood. In this study, we demonstrate important roles of WHSC1L1 in human carcinogenesis. Expression levels of *WHSC1L1* transcript were significantly elevated in various human cancers including bladder carcinoma. Immunohistochemical analysis of bladder, lung, and liver cancers confirmed overexpression of WHSC1L1. *WHSC1L1*-specific small interfering RNAs significantly knocked down its expression and resulted in suppression of proliferation of bladder and lung cancer cell lines. WHSC1L1 knockdown induced cell cycle arrest at the G_2/M phase followed by multinucleation of cancer cells. Expression profile analysis using Affymetrix GeneChip® showed that WHSC1L1 affected the expression of a number of genes including *CCNG1* and *NEK7*, which are known to play crucial roles in the cell cycle progression at mitosis. As WHSC1L1 expression is significantly low in various normal tissues including vital organs, WHSC1L1 could be a good candidate molecule for development of novel treatment for various types of cancer.

INTRODUCTION

DNA–histone complexes comprise the fundamental repeating unit of chromatin and the multiplicity in combinations of histone modifications/nucleosome types results in chromatin-dependent functions. This idea was previously proposed as the "Histone Code Hypothesis" (Strahl and Allis 2000; Turner, 2000; Jenuwein and Allis, 2001). Histones, especially residues of the amino termini of histones H3 and H4 and the amino and carboxyl termini of histones H2A, H2B, and H1, are susceptible to a variety of post-translational modifications such as phosphorylation, acetylation, methylation, ubiquitination, sumoylation, and glycosylation (Margueron et al., 2005). Among histone modifications, methyl-lysine residues in nucleosomal histones are considered to mediate interactions with the macromolecular complexes that regulate chromatin-template processes such as transcription. Despite a large body of information for the prominent role of histone lysine methylation in transcriptional regulation, the involvement of their alterations in human diseases still remains unclear.

We had reported that SMYD3, a histone lysine methyltransferase, stimulated proliferation of cells and played an important role in human carcinogenesis through its methyltransferase activity (Hamamoto et al., 2004, 2006). To investigate possible roles of histone lysine methyltransferases (HKMTases) in human carcinogenesis, we

Additional Supporting Information may be found in the online version of this article.

Supported by: NIHR and the Cambridge Biomedical Research Centre; Japan Society for the Promotion of Science, Grant number: 22681030.

*Correspondence to: Ryuji Hamamoto, Laboratory of Molecular Medicine, Human Genome Center, Institute of Medical Science, The University of Tokyo, 4-6-1 Shirokanedai, Minato-ku, Tokyo 108-8639, Japan. E-mail: ryuji@ims.u-tokyo.ac.jp

Received 2 July 2012; Accepted 20 August 2012
DOI 10.1002/gcc.22012
Published online 25 September 2012 in Wiley Online Library (wileyonlinelibrary.com).

examined the expression profiles of human HKMTases in clinical tissues and found that expression levels of *WHSC1L1* (Wolf–Hirschhorn syndrome candidate—like 1) were significantly up-regulated, compared with their corresponding normal tissues, in various types of cancer. *WHSC1L1*, also known as *NSD3* and *WHISTLE*, shows high sequence similarity to NSD2/*WHSC1* (Wolf–Hirschhorn syndrome candidate-1) and NSD1, particularly in their C-terminal portion, which includes the functional domains (Stec et al., 2001; Douglas et al., 2005). These three NSD proteins form a family of human histone lysine methyltransferases. NSD1, a 2696-amino-acid protein that contains four zinc finger domains, two PWWP (proline-tryptophan-tryptophan-proline) domains, and a SET domain responsible for the HMTase activity, specifically mediates the methyl transfer onto an H3 lysine 36 and H4 lysine 20 (H3K36 and H4K20) (Rayasam et al., 2003; Morishita and di Luccio, 2011). WHSC1 (HKMTase H3K36, H4K20, H3K4, and H3K27) and WHSC1L1 (HKMTase H3K36) share the same functional domains with NSD1 (Li et al., 2009; Morishita and di Luccio, 2011; Wagner and Carpenter, 2012), although the sizes are smaller as 1365 amino acids (NSD2) and 1437 amino acids (NSD3), respectively (Morishita and di Luccio, 2011). Although WHSC1L1 is known to function as a transcriptional regulator that mediates histone methylation (Kim et al., 2006, 2007b), the biological function of the protein has not been well elucidated. Here, we demonstrated a possible involvement of WHSC1L1 in human cancers.

MATERIALS AND METHODS

Bladder Tissue Samples and RNA Preparation

One hundred and twenty surgical specimens of primary bladder carcinoma were collected, either at cystectomy or transurethral resection of bladder tumor (TURBT), and snap-frozen in liquid nitrogen. Twenty-two specimens of normal bladder urothelial tissue were collected from areas of macroscopically normal bladder in patients with no evidence of malignancy. Five sequential sections of 7-μm thickness were cut from each tissue and stained using Arcturus® Histogene® staining solution (Life Technologies, Carlsbad, CA) following the manufacturer's protocol and assessed for cellularity and tumor grade by an independent consultant urohistopathologist. Slides were then transferred for microdissection using a Pix Cell II laser capture microscope (Life Technologies). Additionally, the tumor sections were graded according to the degree of inflammatory cell infiltration (low, moderate, and severe). Samples with high inflammatory cell infiltration were excluded (Wallard et al., 2006). To validate the accuracy of microdissection, primers and probes for Vimentin and Uroplakin were sourced and quantitative reverse transcription polymerase chain reaction (qRT-PCR) performed according to the manufacturer's instructions (Assays on demand, Life Technologies). Vimentin is primarily expressed in mesenchymally derived cells and was used as a stromal marker. Uroplakin is a marker of urothelial differentiation and is preserved in up to 90% of epithelially derived tumors (Olsburgh et al., 2003). Use of tissues for this study was approved by Cambridgeshire Local Research Ethics Committee (Ref. 03/018).

Cell Culture

All cell lines were grown in monolayers in appropriate media: Dulbecco's modified Eagle's medium (DMEM) for EJ28, RERF-LC-AI, Huh-7, and HepG2; Eagle's minimal essential medium for IMR-90, 253J, 253J-BV, HT1197, HT1376, J82, SCaBER, UMUC3, and SBC5 cells; Leibovitz's L-15 for SW780 and SW480 cells; McCoy's 5A medium for RT4, T24, and HCT116 cells; RPMI1640 medium for 5637, A549, H2170, ACC-LC-319, and SNU475 cells supplemented with 10% fetal bovine serum (FBS) and 1% antibiotic/antimycotic solution (Sigma–Aldrich, St. Louis, MO). LoVo cells were cultured in Ham's F-12 medium supplemented with 20% fetal bovine serum and 1% antibiotic/antimycotic solution. Small airway epithelial cells (SAEC) cells were maintained in small airway epithelial cell basal medium supplemented with 52 μg/mL bovine pituitary extract, 0.5 ng/mL human recombinant epidermal growth factor (EGF), 0.5 μg/mL hydrocortisone, 0.5 μg/mL epinephrine, 10 μg/mL transferrin, 5 μg/mL insulin, 0.1 ng/mL retinoic acid, 6.5 ng/mL triiodothyronine, 50 μg/mL Gentamicin/Amphotericin-B (GA-1000), and 50 μg/mL fatty acid-free bovine serum albumin. All cells were maintained at 37°C in humid air with 5% CO_2 condition (IMR-90, SAEC, 5637, 253J, 253JBV, EJ28, HT1197, HT1376, J82, RT4, SCaBER, T24, UMUC3, A549, H2170, ACC-LC-319, RERF-LC-AI, SBC5, 293T, HepG2, SNU475, Huh-7, and LoVo) or without CO_2 (SW780 and SW480). Cells were transfected with

FuGENE6™ (Roche Applied Science, Penzberg, Germany) according to manufacturer's protocols (Cho et al., 2011b).

Expression Profiling in Cancer Using cDNA Microarrays

We established a genome-wide cDNA microarray with 36,864 cDNAs selected from the UniGene database of the National Center for Biotechnology Information. This microarray system was constructed essentially as described previously (Kitahara et al., 2001; Kikuchi et al., 2003; Nakamura et al., 2004). Briefly, a total of 30,000–40,000 cancer or noncancerous cells were collected selectively using the EZ cut system (Molecular Machines & Industries, Glattbrugg, Switzerland) according to the manufacturer's protocol. Extraction of total RNA, T7-based amplification, and labeling of probes were performed as described previously (Kitahara et al., 2001). A measure of 2.5-μg aliquots of twice-amplified RNA (aRNA) from each cancerous and noncancerous tissue was then labeled, respectively, with Cy3-dCTP and Cy5-dCTP. Detailed expression profiling data shown in this study were based on the data reported previously (Kaneta et al., 2003; Kikuchi et al., 2003; Takata et al., 2005).

Quantitative Real-Time PCR

As described previously, we prepared 120 bladder cancer and 22 normal bladder tissues in Cambridge Addenbrooke's Hospital. For quantitative RT-PCR reactions, specific primers for all human *GAPDH* (housekeeping gene), *SDH* (housekeeping gene), and *WHSC1L1* were designed (primer sequences in Supporting Information, Table S1). PCR reactions were performed using the ABI prism 7700 Sequence Detection System (Life Technologies) following the manufacture's protocol. 50% SYBR GREEN universal PCR Master Mix without UNG (Life Technologies), 50 nM each of the forward and reverse primers, and 2 μL of reverse transcriptional cDNA were applied. Amplification conditions were first 5 min at 95°C and then 45 cycles each consisting of 10 sec at 95°C, 1 min at 55°C and 10 sec at 72°C. After this, samples were incubated for 15 sec at 95°C, 1 min at 65°C to draw the melting curve, and cooled to 50°C for 10 sec. Reaction conditions for target gene amplification were as described earlier, and 5 ng of reverse transcribed RNA was used in each reaction.

Immunohistochemical Staining

Immunohistochemical analysis was done using anti-WHSC1L1 antibody (1:500, 11345-1-AP, Proteintech, Chicago, IL) as described previously (Takawa et al., 2011; Toyokawa et al., 2011a–c). For clinical bladder and lung cancer tissue microarray, EnVision kit/horseradish peroxidase (Dako, Carpinteria, CA) was applied. Briefly, slides of paraffin-embedded tumor specimens were processed under high pressure (125°C, 30 sec) in antigen-retrieval solution, high pH 9 (S2367; Dako), treated with peroxidase blocking regent, and then treated with protein blocking regent (X0909; Dako). Tissue sections were incubated with a rabbit anti-WHSC1L1 polyclonal antibody followed by secondary antibodies conjugated to peroxidase labeled dextran polymers (Dako). Antigen was visualized with substrate chromogen (Dako liquid DAB chromogen; Dako). Finally, tissue specimens were stained with Mayer's haematoxylin (Hematoxylin QS, Vector Laboratories, Burlingame, CA) to discriminate the nucleus from the cytoplasm. Because the intensity of staining within each tumor tissue core was mostly homogeneous, the intensity of WHSC1L1 staining was semiquantitatively evaluated using the following criteria: negative (no appreciable staining in tumor cells) and positive (brown staining appreciable in more than 30% of the nucleus of tumor cells).

siRNA Transfection

siRNA oligonucleotide duplexes were purchased from SIGMA Genosys for targeting the human *WHSC1L1* transcript. siEGFP and siNegative control (siNC), which is a mixture of three different oligonucleotide duplexes, were used as control siRNAs. The siRNA sequences are described in Supporting Information, Table S2. siRNA duplexes (100 nM final concentration) were transfected into bladder and lung cancer cell lines with Lipofectamine 2000 (Life Technologies) for 72 hr, and cell viability was examined using the Cell Counting Kit-8 (Dojindo, Kumamoto, Japan).

Flow Cytometry Assay

SBC5 and SW780 cells were treated with siWHSC1L1 or control siRNAs (siEGFP and siNC) and cultured in a CO_2 incubator at 37°C for 72 hr. Aliquots of 1×10^5 cells were collected by trypsinization and stained with propidium iodide (PI) following the manufacturer's instructions (Cayman Chemical). Cells were analyzed by

FACScan (Beckman Coulter, Brea, CA) with MultiCycle for Windows software (Beckman Coulter) for detailed cell cycle status. The percentages of cells in G_0/G_1, S, and G_2/M phases of the cell cycle were determined from at least 20,000 ungated cells.

Western Blot

Whole cell lysates were prepared from the cells with CelLytic^{TM} M buffer, and total protein was transferred to nitrocellulose membrane. The membrane was probed with an anti-WHSC1L1 antibody (11345-1-AP, Proteintech) and an anti-ACTB antibody (RB-9421, Thermo Fisher Scientific, Waltham, MA). ACTB was served as an internal control. Protein bands were detected by incubating with horseradish peroxidase-conjugated antibodies (GE Healthcare, Little Chalfont, UK) and visualizing with Enhanced Chemiluminescence (GE Healthcare).

Clonogenicity Assays

COS7 cells, cultured in DMEM 10% FBS, were transfected with a pCAGGS-n3FC empty vector or a pCAGGS-n3FC-WHSC1L1 (Full-length WHSC1L1 protein expression) vector. The transfected COS7 cells were cultured for 2 days and seeded in 10-cm dish at the density of 10,000 cells per 10-cm dish in triplicate. Subsequently, the cells were cultured in DMEM 10% FBS containing 0.4 (mg/mL) Geneticin/G-418 for 2 weeks until colonies were visible. Colonies were stained with Giemsa (MERCK, Whitehouse Station, NJ) and counted by Colony Counter software.

Coupled Cell Cycle and Cell Proliferation Assay

A 5′-bromo-2′-deoxyuridine (BrdU) flow kit (BD Pharmingen, San Diego, CA) was used to determine the cell cycle kinetics and to measure the incorporation of BrdU into DNA of proliferating cells. The assay was performed according to the manufacturer's protocol. Briefly, cells (1×10^6 per well) were seeded overnight in 10-cm diameter Petri dishes and treated with an optimized concentration of siRNAs in medium containing 10% FBS for 72 hr, followed by addition of 10 μM BrdU, and incubations continued for an additional 30 min. Both floating and adherent cells were pooled from triplicate wells per treatment point, fixed in a solution containing paraformaldehyde and the detergent saponin, and incubated for 1 hr with DNase at 37°C (30 μg per sample). Fluorescein isothiocyanate (FITC)-conjugated anti-BrdU antibody (1:50 dilution in Wash buffer; BD Pharmingen) was added and incubation continued for 20 min at room temperature. Cells were washed in Wash buffer and total DNA was stained with 7-amino-actinomycin D (7-AAD; 20 μL per sample), followed by flow cytometric analysis using FACScan (Beckman Coulter), and total DNA content (7-AAD) was determined CXP Analysis Software Ver. 2.2 (Beckman Coulter).

Microarray Hybridization and Statistical Analysis for the Clarification of Down-Stream Genes

Total RNAs were purified from A549 and SW780 cells 24 hr after treatment with siRNAs. Samples were labeled and hybridized onto Affymetrix GeneChip U133 Plus 2.0 oligonucleotide arrays (Affymetrix, Santa Clara, CA) according to the manufacturer's instructions. The statistical procedure for micaroarray analysis was described preciously (Hayami et al., 2010, 2011; Cho et al., 2011a; Yoshimatsu et al., 2011). We also performed a pathway analysis using the hypergeometric distribution test, which calculates the probability of overlap between the up/down-regulated gene set and each GO category compared against another gene list that is randomly sampled. We applied the test to the identified up/down-regulated genes to test whether or not they are significantly enriched false discovery rate (FDR) ≤ 0.05) in each category of "Biological processes" (857 categories) as defined by the Gene Ontology database.

RESULTS

Overexpression of WHSC1L1 in Clinical Cancer Tissues

We examined expression levels of histone lysine methyltransferase genes in a small number of clinical bladder cancer samples and found *WHSC1L1* to be significantly overexpressed in the cancer cells compared with the corresponding noncancerous tissues (data not shown). We then analyzed 120 bladder cancer samples and 22 normal controls and confirmed significant elevation of the *WHSC1L1* expression in tumor cells compared with normal cells ($P < 0.0001$, Mann–Whitney U test, Fig. 1A). We subclassified these tumors according to metastasis and recurrence status as well as gender or smoking history but found no difference in their expression level by these parameters (Table 1). In addition, our previous microarray expression

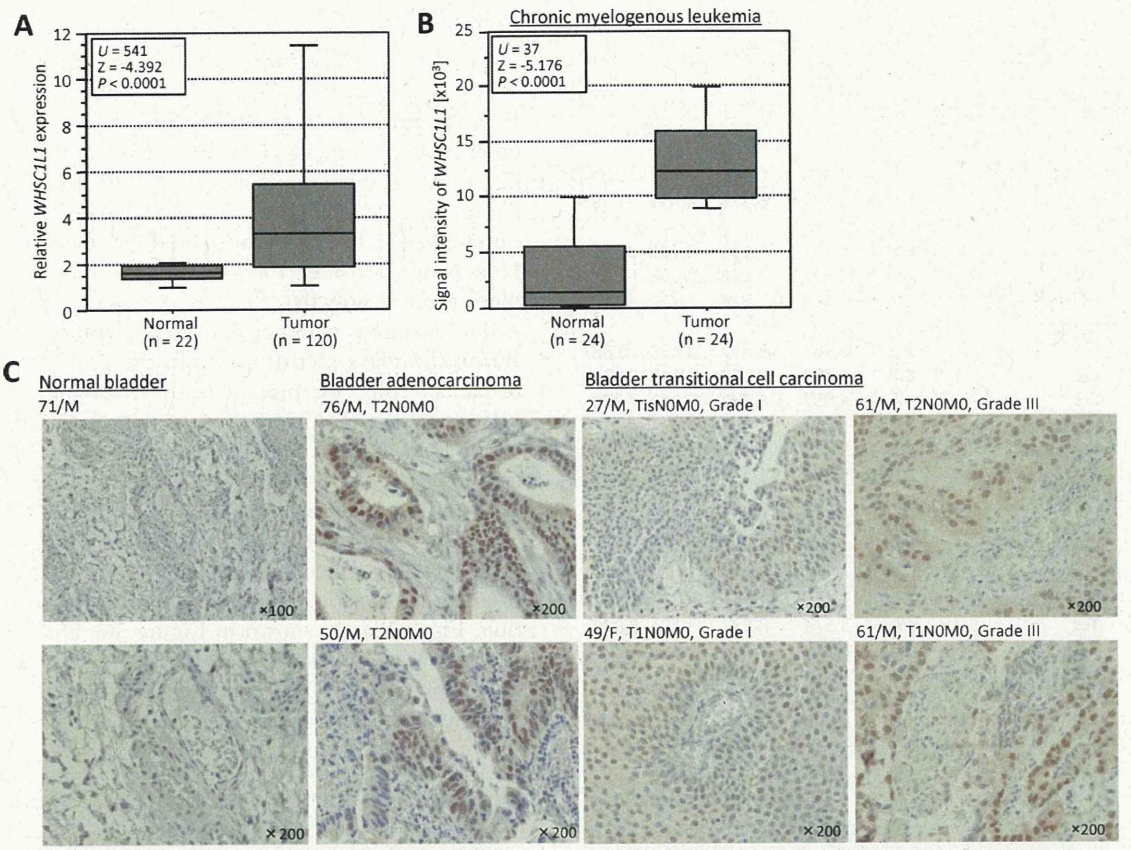

Figure 1. Elevated WHSC1L1 expression in human cancers. (A) Expression levels of *WHSC1L1* were analyzed by quantitative real-time PCR, and the result is shown by box-whisker plot (median 50% boxed). Relative mRNA expression shows the value normalized by *GAPDH* and *SDH* expressions. Mann–Whitney *U* test was used for statistical analysis. (B) Expression analysis of *WHSC1L1* in CML. Signal intensity of each sample was analyzed by cDNA microarray, and the result is shown by box-whisker plot (median 50% boxed). Mann–Whitney *U* test was used for the statistical analysis. (C) Immunohistochemical staining of WHSC1L1 in bladder tissues. Counterstaining was done with hematoxylin. Original magnification, 100× and 200×.

analysis of a large number of clinical samples (Kaneta et al., 2003; Kikuchi et al., 2003) indicated that *WHSC1L1* expression was significantly up-regulated in chronic myelogenous leukemia (CML; Fig. 1B) and other types of tumor (Supporting Information, Fig. S1). To confirm elevated WHSC1L1 expression levels in bladder tissues at the protein level, we validated the specificity of an anti-WHSC1L1 antibody as shown in Supporting Information, Figure S2A. We then performed immunohistochemical analysis using this antibody and observed much stronger WHSC1L1 staining in the nucleus of malignant cells than in non-neoplastic tissues (Fig. 1C). Among 29 bladder cancer tissue sections, we detected its positive staining in 19 cases (65.5%; Supporting Information, Table S3). However, we found no relationship between WHSC1L1 protein expression levels and clinicopathologic characteristics, consistent with our real-time PCR results shown earlier. Because our previous cDNA microarray data implicated its overexpression in lung cancer, we conducted immunohistochemical analysis using clinical lung tissues and confirmed WHSC1L1 overexpression in cancer cells at the protein level (Fig. 2A). We also examined expression levels of WHSC1L1 in various histological types of lung tumor tissues by tissue microarray. Of 61 lung tumors examined, we observed strong staining in 43 cases (70.5%; Fig. 2A and Supporting Information, Table S4). We additionally performed tissue microarray analysis of WHSC1L1 in liver cancer tissues (Fig. 2B and Supporting Information, Table S5) and found significant staining in 31 cases (47.0%) of 66 liver cancers, while the staining was hardly detectable in the remaining 35 cancers as well as normal liver and viral hepatitis related cirrhosis, indicating that WHSC1L1 is frequently overexpressed in various types of cancer.

TABLE 1. Statistical Analysis of *WHSC1L1* Expression Levels in Clinical Bladder Tissues

		WHSC1L1		
Characteristic	Case (*n*)	Mean	SD	95%CI
Normal (control)	22	1.593	0.397	1.427–1.759
Tumor (total)	120	5.537	8.376	4.039–7.036
Tumor stage				
pTa, pT1	85	6.181	9.670	4.125–8.236
pT2	25	4.527	3.658	3.093–5.961
pT3, pT4	6	3.169	1.814	1.717–4.620
Tumor grade				
G1	12	6.987	6.892	3.088–10.887
G2	60	5.782	8.458	3.642–7.922
G3	47	4.857	8.792	2.343–7.370
Metastasis				
Negative	93	5.433	7.412	3.926–6.939
Positive	27	5.898	11.251	1.654–10.142
Gender				
Male	88	6.155	9.453	4.179–8.130
Female	30	3.727	3.908	2.329–5.126
Recurrence				
No	27	7.635	11.681	3.229–12.041
Yes	49	5.574	8.832	3.101–8.046
Died	8	8.263	8.403	2.441–14.086
Smoke				
No	27	6.446	6.318	4.063–8.828
Yes	48	6.509	12.013	3.110–9.907

WHSC1L1 Regulates the Growth of Cancer Cells

To investigate the oncogenic activity of WHSC1L1, we conducted a clonogenicity assay. Either a WHSC1L1 expression vector or an empty vector (mock) was transfected into COS-7 cells. As shown in Figure 3A, COS-7 cells expressing WHSC1L1 showed higher colony numbers than mock-transfected COS-7 cells. Hence, we consider that WHSC1L1 might promote the cell growth.

To examine whether elevated expression of *WHSC1L1* plays a critical role in the proliferation of cancer cells, we prepared siRNA oligonucleotide duplexes that were designed to specifically suppressed the expression of *WHSC1L1* (siWHSC1L1#1, #2) and transfected either duplex into bladder and lung cancer cell lines. We first confirmed high expression levels of WHSC1L1 in cancer cell lines at the mRNA and protein levels (Fig. 3B and Supporting Information, Fig. S2B). As shown in Figure 3C, both siRNAs for WHSC1L1 suppressed the expression of the corresponding genes, while no effect was observed when we treated the cells with siEGFP

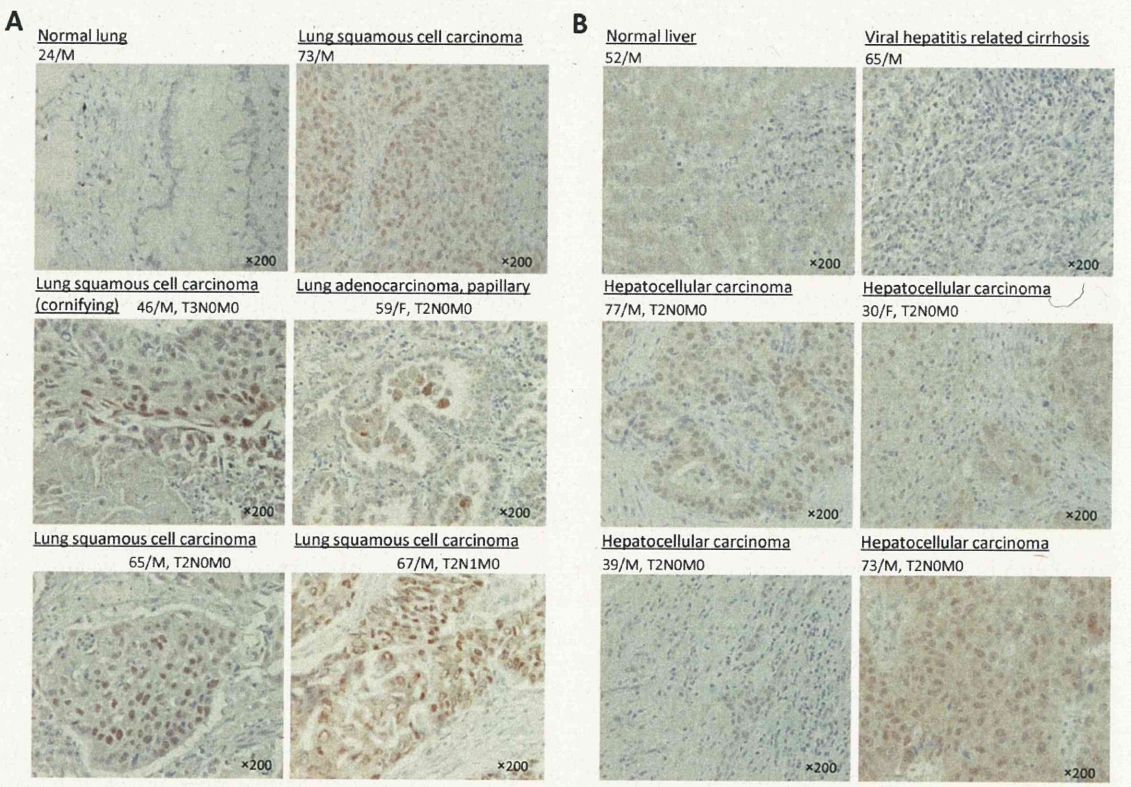

Figure 2. Tissue microarray images of clinical lung tissues (A) and liver tissues (B) stained by standard immunohistochemistry for protein expression of WHSC1L1. Clinical information for each section is represented above histological pictures. All tissue samples were purchased from BioChain. Original magnification, 200×.